Proceedings 10th NUMGE 2023
10th European Conference on Numerical Methods in Geotechnical Engineering
Zdravkovic L, Kontoe S, Taborda DMG, Tsiampousi A (eds)

https://doi.org/10.53243/NUMGE2023-410

Seismic Response of a Buried Pipeline in Sandy Soil Layer: Numerical Approach

S Sahoo[1], and B Naveen[2]

[1] *Assistant Professor, Department of Civil Engineering, National Institute of Technology, Meghalaya, Meghalaya, INDIA, 793003*

[2] *Research Scholar, Department of Civil Engineering, National Institute of Technology, Meghalaya, Meghalaya, INDIA, 793003*

ABSTRACT: Researches from the past indicated that buried pipelines are at higher risk to failure when exposed to seismic conditions because of the high probability of destruction, damage, and disruption under such conditions. In this study, earthquake time-history analyses were carried out on a buried pipeline of API 5L Grade X70, which is commonly used for oil and gas transmission. To investigate the influence of earthquakes on the buried pipeline, a set of numerically created models were studied on a pipeline system buried in sandy soil with various peak ground acceleration (PGA) of 0.24g, 0.46g, and 0.77g. A systematic study is carried out to determine the soil displacement, strain, acceleration, and displacement of pipelines buried in two different soil conditions (loose sand and dense sand). Analyses are also being done on the acceleration response of loose sand and dense sand. Overall, the research suggests that dense sand de-amplify the original ground motion while loose sand amplify it. The findings show that earthquakes are more likely to cause damage to pipeline if they are buried in loose sand. Therefore, the current study provides useful information that should be included in the seismic design of buried pipelines.

Keywords: Buried pipeline; Seismic response; Loose sand; Dense sand; Acceleration amplification factor.

1 INTRODUCTION

In the daily routines of human life, pipes have always been extremely important. These pipes are sometime known as "lifeline systems" due to their importance in maintaining property and life sustenance. Pipelines are frequently constructed underground and are referred as buried pipelines (Ariman and Muleski, 1981). Water and wastewater facilities, transmission lines for liquid fuels and natural gas, and lines for electricity and communications are all provided by buried pipes (Novak and Hindy, 1980; Tseng et al., 2010). After being exposed to dynamic loading circumstances like an earthquake, they often play a significant part in contemporary life as well as in disaster control and mitigation (Maotian et al., 2009; Zhang et al., 2011). Both permanent and transient ground deformations, which are caused by earthquakes, have the potential to damage buried pipelines. Elhmadi and O'Rourke, 1990 provided a summary as well as a discussion of the primary factors contributing to permanent ground deformation (PGD). Landslides, liquefaction, densification of loose granular deposits, faulting, tectonic uplift, and subsidence are also included in this category (Yan et al., 2012). It has been found that during an earthquake, these buried pipelines are vulnerable and the damages and disruptions of these buried pipelines can lead to the loss of vital services or more precisely lifeline services. Failure of these buried pipelines such as oil and gas pipelines may lead to detrimental effects on the environment and the people (Flores-Berrones and Liu, 2003; Mishra, 2016). There were many cases where pipelines were heavily damaged by strong earthquakes and experienced lifeline failures such as the 1971 San Fernando earthquake which only affected 1 % of the region due to surface faulting but caused over 1400 breaches in water, natural gas, and sewer pipes (Novak, 1974). In total, 234 distinct areas had gas leaks from underground pipelines as a result of the Kobe earthquake in Japan in 1995. The 1999 Chi-Chi earthquake in Taiwan caused the Chelungpu fault to rupture which ultimately caused severe damage to the buried pipelines. It completely destroyed a water supply facility in the area near the fault line (Chen et al., 2001). In 2000, the distribution and service pipeline at 892 locations within the service area of Yonago was completely damaged by the Tottoriken-Seibu earthquake (Umeda, 2002).

Granular materials, like sands, can densify when subjected to earthquake loading. The presence of pore fluids prevents the volume from decreasing in saturated deposits. As earthquake is a quick loading phenomenon, it does not facilitate adequate drainage even in granualr soil instead increases the pore water pressure for a short duration, which leads to a state that is almost completely undrained. The tendency for the volume of the soil skeleton to shrink under this undrained situation raises the pore fluid pressure (Saeedzadeh and Hataf, 2011). As a result, these cohesionless soils have lower effective stress and hence lower shear resistance. As long as excess pore fluid pressure is generated, liquefaction may take place as the effective stress steadily decreases. Excess pore water pressure beneath the pipeline and reduced shear resistance of the soil above it cause the pipeline to float (Ariman and Muleski, 1981; Badv and Daryani, 2010; Nair and Dash, 2015). The amplitude, frequency content, and duration of significant ground motion are all strongly impacted by local site factors. The magnitude of their influence is mainly dependent on the subsurface's material qualities (Kumar et al., 2022).

Considering these insights and constraints, a set of numerically created models were analyzed in the present study on a pipeline system buried in sandy soil with different peak ground acceleration (PGA) to examine the effect of earthquakes on the buried pipeline. A methodical study is done on soil displacement, strain, acceleration, and displacement of pipelines buried in two different soil condition (loose sand and dense sand). Analyses are also being done on acelearation amplification coefficient of loose sand and dense sand at a different loading level of ground motion under unidirectional consistent excitation.

2 DETAILS OF NUMERICAL MODELLING

The Finite Element (FE) model of the buried pipeline is modelled with the MIDAS GTS NX 2021 (*v1.1*). In this particular investigation, an API 5L-X70 steel pipeline is considered (American Petroleum Institute in Washington, DC). The API 5L-X70 pipeline was mostly used to transport oil and gas. This particular pipeline had a length of 50 m. The pipe is modelled as an elastic two-dimensional plate structure. In the model, gravelly soil is placed around the hollow steel pipeline. The pipe is buried at a depth of 2.1 m from the ground surface. Table 1 gives a summary of the material properties of the chosen buried pipeline. Three assumptions were made when the modelling of the pipeline was set up. First, the live load on the surface of the ground is not taken into account. Second, the pipe is buried above the level of the groundwater. Third, two types of soil conditions- Loose sand (ϕ=25° denoted as LS), and Dense sand (ϕ=35° denoted as DS) are considered. The Mohr-coulomb model is utilized to explain the elasto-plastic behavior of soil because it does so in a more precise manner, particularly when it comes to reflecting the friction and support effects of soil on the pipeline. The detailed material properties of soil used in this FE analysis are shown in Table 2. In this model, normal stiffness modulus (K_n) and shear stiffness modulus (K_t), adhesion, interface friction angle and the assumed strength reduction factor from the material properties of soil and pipe properties are provided as the interface between gravel and pipeline.

In this study, the damping constants i.e., 'c_p' and 'c_s' required for the time-history analysis are calculated as follows (Midas GTS NX (340) 2023 v1.1):

$$C_p = \rho \cdot A \cdot \sqrt{\frac{\lambda+2G}{\rho}} = W \cdot A \cdot \sqrt{\frac{\lambda+2G}{W \cdot 9.81}} = c_p \cdot A \qquad (1)$$

$$C_s = \rho \cdot A \cdot \sqrt{\frac{G}{\rho}} = W \cdot A \cdot \sqrt{\frac{G}{W \cdot 9.81}} = c_s \cdot A \qquad (2)$$

Where, $\lambda = \frac{\nu E}{(1+\nu)(1-2\nu)}$; $G = \frac{E}{2(1+\nu)}$

A: Cross-sectional area (m^2); E: Modulus of elasticity (kN/m^2)
W: Unit weight (kN/m^3); λ: Volumetric modulus of elasticity (kN/m^2)
G: Shear modulus (kN/m^2); ν: Poisson's ratio

In the FE analyses, the meshing for the soil elements was done using 10-noded tetrahedron elements, meshing for the plate components of the pipeline was done using 8-noded quadratic elements. The model meshed in such a way that the sizes of the mesh are finer around the pipeline than the rest part of the model as shown in Figure 1. In this model, the bottom boundary is fixed and for the sides, viscous boundary conditions are applied. Linear time-history analyses were carried out with PGA of 0.24g, 0.46g, and 0.77g provided as unidirectional seismic excitation (along the lateral direction of the pipeline orientation). An Eigen value analysis was conducted on the embedded pipeline under various soil conditions. This eigen value analysis is used to analyze the inherent dynamic properties of the ground/structure, and this can be used to obtain the natural mode (mode shape), natural period (natural frequency), and modal participation factor of the ground/structure. The natural time periods for the first two modes of vibrations in dense sand are 0.94s and 0.98s respectively. In case of loose sand, it is 1.17s and 1.20s respectively.

3 RESULTS AND DISCUSSION

3.1 Displacement in pipe and soil

During an earthquake, usually there is a relative shear deformation between the pipeline and the soil. This kind of distortion adversely affects the surface of the buried pipeline which lead to the pipeline's deformation and destruction. Figure 2 represents the maximum relative displacement response of the straight pipeline when subjected to a variety of seismic ground motions. It is observed that a similar response is projected for the various soil conditions along the pipeline length. The overall maximum relative displacement in dense sand is raised from 10 mm to 28 mm as a result of an increase in PGA from 0.24g to 0.77g. When loose sand is considered, the total maximum relative displacement of the pipeline increases from 12 mm to 37 mm.

Most of the time, the maximum displacement response is mostly at the center of the pipeline. Compared to dense sand, pipe displacement is greater in loose sand because soil displacement is greater in loose sand. Dense sand has a less effect on pipe displacement.

Figure 3 represents the total soil displacement curve. Under consistent unidirectional excitation, the gradient of the soil displacement curve keep increasing as the level of input loading of ground motion increases.

Table 1. Material properties of the API 5L Grade X70 buried pipeline.

Pipe	Modulus of Elasticity (E), kN/m^2	Unit Weight (γ), kN/m^3	Outer Diameter, mm	Thickness, mm	Model type
API 5L-X70	206892900	76	2100	15	Elastic

Table 2. Soil material properties

Parameters	Dense sand	Loose sand	Gravel
Modulus of Elasticity (E), kN/m^2	4000	2500	18000
Poisson's Ratio (v)	0.35	0.35	0.33
Unit Weight (γ), kN/m^3	19	17.5	19.5
Cohesion (c), kN/m^2	0	0	0
Frictional angle (ϕ)	35°	25°	40°
Model Type	Mohr-Coulomb	Mohr-Coulomb	Mohr-Coulomb

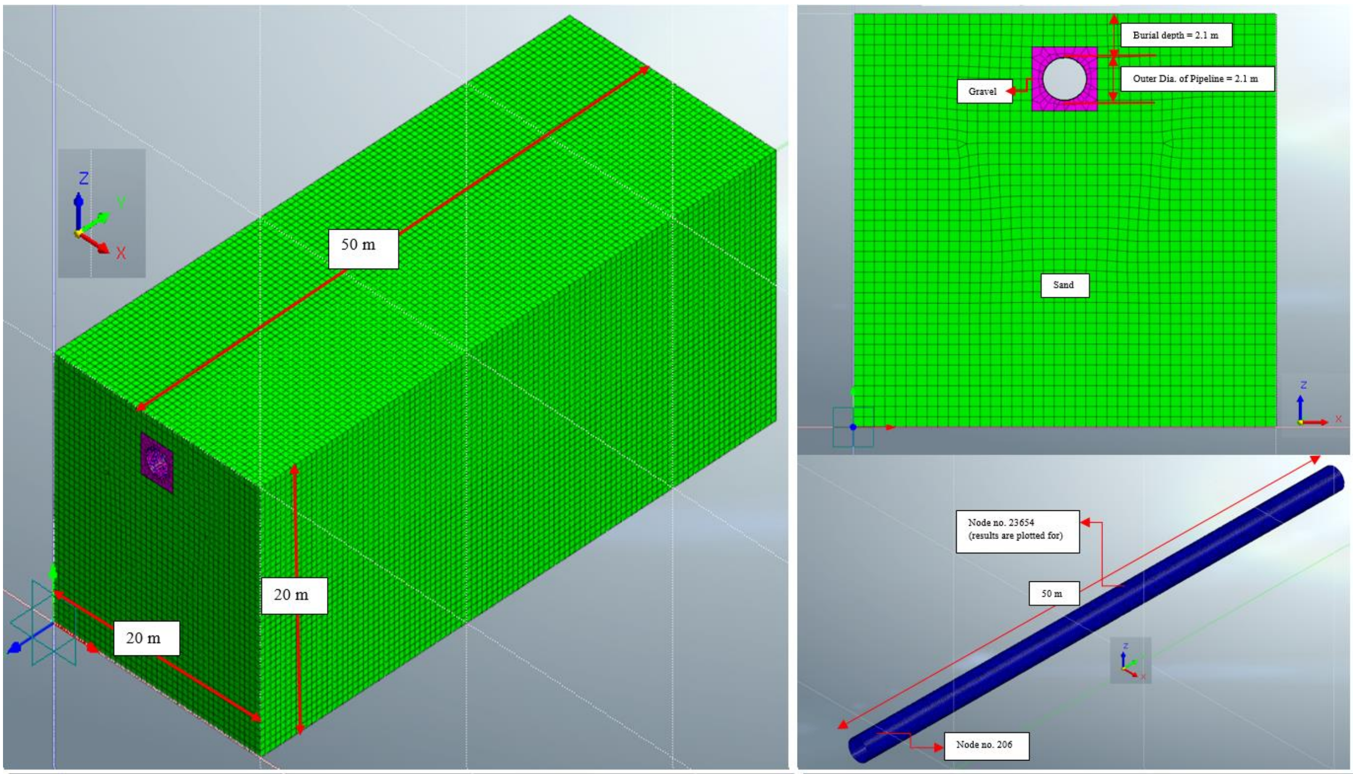

Figure 1. FE modelling of a buried pipeline system. (a) A view of entire model in three dimensions (b) A frontal XZ plane view of the entire model and (c) A view of the pipeline in three dimensions

The maximum total displacement of dense sandy soil is 17 mm, 32 mm, and 42 mm when the input loading level of ground motion is 0.24g, 0.46g, and 0.77g respectively. When the same amount of ground motion is applied to the ground, the total displacement in loose sandy soil is 24 mm, 40 mm, and 56 mm respectively. This suggests that the shear effect of the soil is greater in loose sand and that it also increases with an increase in the loading magnitude of ground motion.Analysis of acceleration response of soil and pipeline

3.1.1 Acceleration response of soil

The acceleration amplification factor (AAF) for DS and LS at a different loading level of ground motion under unidirectional consistent excitation is shown in Figures 4 and 5, respectively.

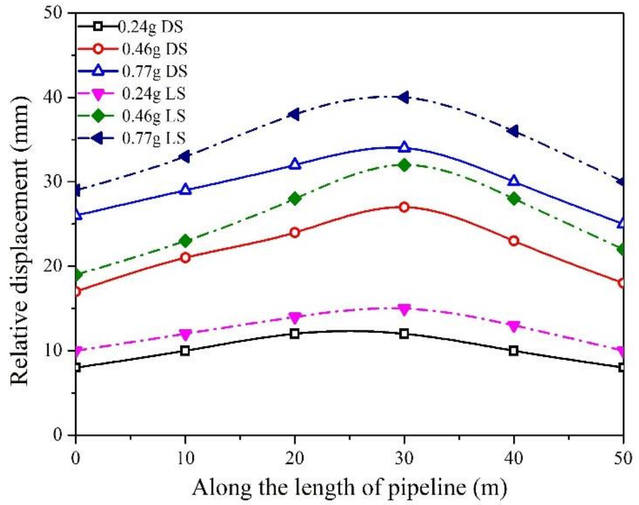

Figure 2. Relative displacement curve along the length of pipeline

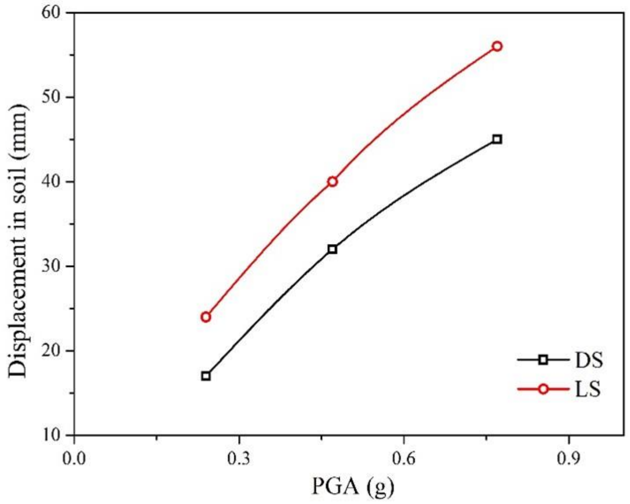

Figure 3. Total displacement in soil

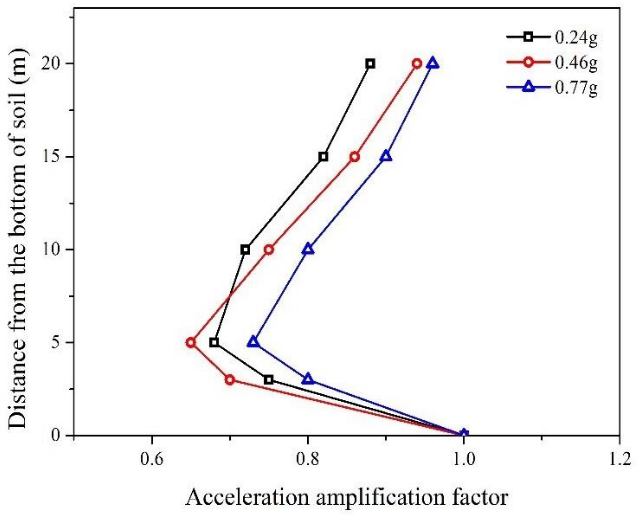

Figure 4. Acceleration amplification factor in dense sand

Figure 4. illustrates dense sand deamplify the acceleration period and the soil acceleration amplification factor 1st decreases and then increases but the AAF value always remained below 1. This suggests that when the input ground motion is applied at the bottom most ground level, the nearby soil gets densified further but while propagating further towards upper part of soil, the soil grains dilates soon after achieving the densest state which generate the appearance of surface cracks.

The AAF at the bottom to the top of the dense sand ranges from 0.7 to 0.9 under unidirectional continuous stimulation at a loading intensity of 0.24*g* ground motion. The AAF ranges from 0.68 to 0.94 at a loading intensity of 0.46*g* ground motion. Similarly, the AAF of dense sand from bottom to top ranges from 0.75 to 0.95 for a loading intensity of 0.77*g* ground motion. Although the values of AAF keep on increasing from bottom most level of soil stratum to the ground surface but the maximum value remain less than 1 which is a clear indication of de-amplification of accleration response to all kinds of seismic excitation under study.

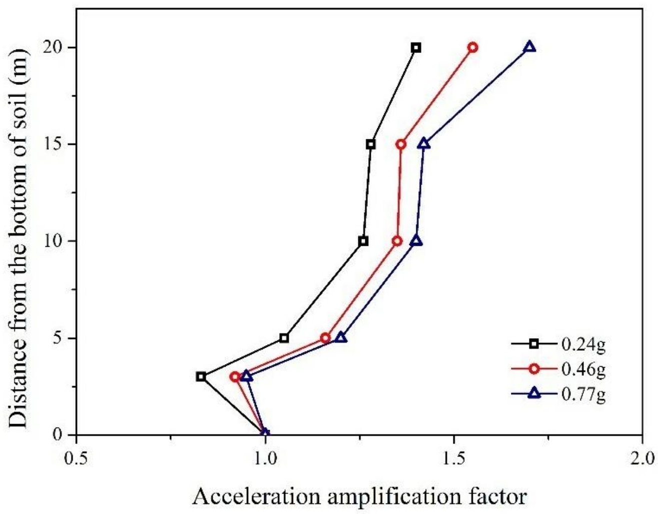

Figure 5. Acceleration amplification factor in loose sand

Figure 5 illustrates, loose sand amplify the acceleration period. It is a clear indication that the AAF initially diminishes up to 3 m from the ground level where seismic excitation was applied and then increases continuously towards the top surface of the ground. This can be due to the densification of the loose granular soil near the seismic load application location because of which the soil near the bottom surface behaves in a similar way to that of dense granualar soil. But, soon after attaining a distance of 3 m from bottom, the seismic waves travel in original loose granular state of soil and shows the true nature of amplification.

Under unidirectional consistent excitation at a loading intensity of 0.24*g* ground motion, the AAF in loose sand from bottom most soil level to the ground surface increases from 0.94 to 1.3. Similarly, the AAF increases from 0.97 to 1.35 at a load intensity of 0.46*g*. And, the AAF at a loading intensity of 0.77*g* increases from 0.98 to 1.75. Hence, it can be concluded that the loose sand amplifies the acceleration response to all the seismic excitations under study.

As per IS1893-Part 1 (2002), response spectra are used to describe the PGA. A soil-specific response analysis is performed to validate the applicability of the response spectra. The comparison of the input and output response spectra provides a clear picture of whether the soil has an amplifying or dampening effect on the ground motion (Bureau of Indian Standards, New Delhi, 2002). The response spectrum of 0.24*g* ground motion and the response spectrum of DS and LS with 5% damping are shown in Figure 6. It shows that the response spectrum of LS is above the original ground motion response spectrum, but in the case of DS, it is below the original response spectrum.

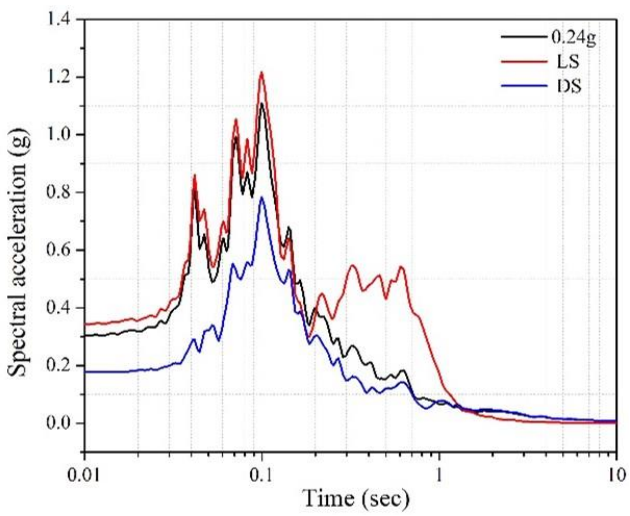

Figure 6. Graph of Response spectrum of input ground motion and different soil condition

3.1.2 Acceleration response of pipeline

Figure 7 depicted the fourier spectrum of longitudinal acceleration at the node point of 206 (as shown in Figure 1 (c)) in the pipeline under unidirectional consistent excitation. It can be observed that the fourier spectrum of the pipeline is essentially the same for the loading intensity of 0.24*g* in both DS and LS when subjected to consistent excitation.
In the case of DS, the longitudinal acceleration fourier amplitude of the pipe is smaller than the input acceleration (i.e., 0.24*g*). However, in case of LS, it is greater than the input acceleration. This can be because of the fact that LS amplify the ground acceleration and DS de-amplify it. This phenomena demonstrates that the site soil has a significant influence on the seismic behaviour of pipeline, and that the acceleration of the pipeline is susceptible to the acceleration of the site soil.

3.2 Analysis of strain in the pipeline

Figure 8 illustrate the longitudinal strain that was induced in the pipeline both in case of DS and LS. The maximum longitudinal strain that was induced in the pipe was found at one-fourth the length of the pipeline in both soil conditions. It should come as no surprise that the amount of strain created in the pipe would increase as the intensity of the ground motion increases.

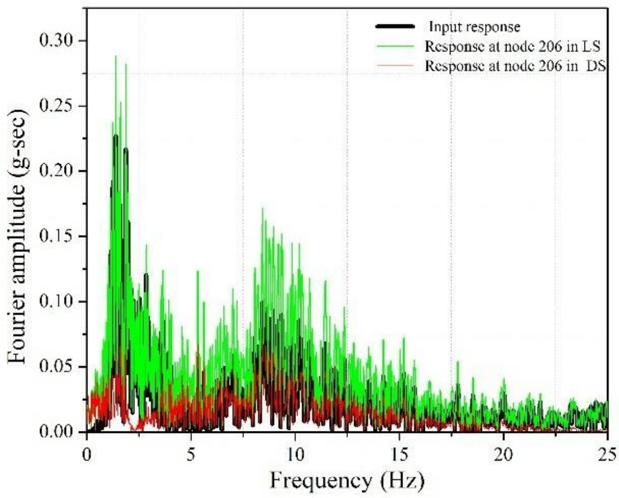

Figure 7. Fourier amplitude of the pipeline under 0.24g ground motion in DS and LS

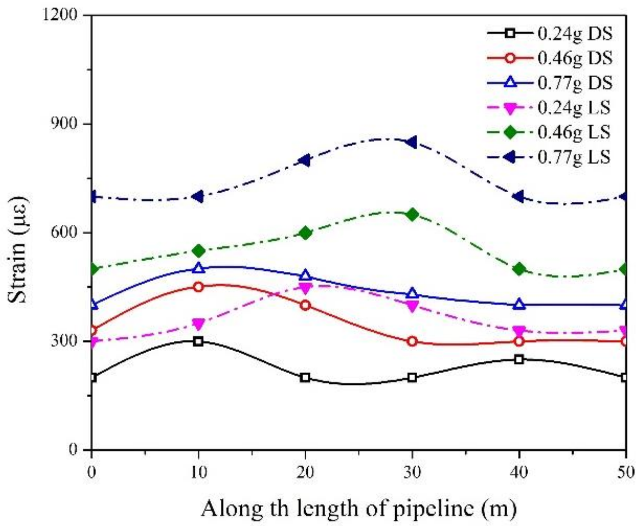

Figure 8. Longitudinal strain along the length of pipeline in the DS and LS

In case of pipeline buried in loose sand maximum longitudinal strain induced in pipe at PGA of 0.24*g*, 0.46*g*, and 0.77*g* are 252 $\mu\varepsilon$, 405 $\mu\varepsilon$, and 512 $\mu\varepsilon$ respectively. At the same loading level of ground motion, maximum longitudinal strain induced in pipeline buried in dense sand are 367 $\mu\varepsilon$, 542 $\mu\varepsilon$, and 713 $\mu\varepsilon$ respectivly. As can be seen from the figures, the strain that is generated in a pipeline that is buried in dense sand is greater than the strain that is produced in a pipeline that is buried in loose sand under the same loading level. This is because the peak acceleration that the soil initially experienced gets amplified and/or de-amplified by the soil.

4 CONCLUSIONS

This research investigates the seismic behaviour of buried pipelines embedded in LS and DS under unidirectional consistent excitation. By examining variation in soil and pipe displacement, soil and pipe acceleration, and strain caused in buried pipe, the following results are drawn.

1. The maximum relative displacement response is mostly in the middle of the pipeline, and the displacement of loose sand is 1.4 times that of dense sand. This shows that the shear effect of soil is higher in loose sand, which will damage the pipeline more.
2. The acceleration of the pipeline is dependent on the acceleration of the soil that surrounding it. According to the findings, loose sand has the effect of amplifying the initial acceleration, whereas dense sand has the opposite effect of de-amplifying it. The findings suggest that pipe is expected to be damaging to loose sand. However, the amplification property of any soil is affected by the thickness of the layer, the location of the water table, and the type of underlying layer. The acceleration amplification factor of loose sand ranges from 0.95 to 1.7, while that of dense sand ranges from 0.65 to 0.95. These data can be used to recommend design response spectra values for sandy soil.
3. The variation in the pipeline strain curve caused by the various ground motions in DS and LS is the same. When compared to the maximum longitudinal strain created in pipe when buried in DS, the maximum longitudinal strain induced in pipe when buried in LS is 1.45 times greater. Overall, the results show that pipelines buried in loose sand are more likely to be damaged by earthquakes.

5 REFERENCES

Ariman, T., & Muleski, G. E. (1981). A review of the response of buried pipelines under seismic excitations. *Earthquake Engineering & Structural Dynamics*, *9*(2), 133–152. https://doi.org/10.1002/eqe.4290090204

Badv, K., & Daryani, K. E. (2010). An investigation into the upward and lateral soil-pipeline interaction in sand using finite difference method. *Iranian Journal of Science and Technology, Transaction B: Engineering*, *34*(4), 433–445.

Bureau of Indian Standards New Delhi. (2002). Criteria for Earthquake Resistant Design of Structures - General Provisions and Buildings Part-1. *Bureau of Indian Standards, New Delhi*, *Part 1*(1), 1–39.

Chen, W. S., Huang, B. S., Chen, Y. G., Lee, Y. H., Yang, C. N., Lo, C. H., Chang, H. C., Sung, Q. C., Huang, N. W., Lin, C. C., Sung, S. H., & Lee, K. J. (2001). 1999 Chi-Chi earthquake: A case study on the role of thrust-ramp structures for generating earthquakes. *Bulletin of the Seismological Society of America*, *91*(5), 986–994. https://doi.org/10.1785/0120000731

Elhmadi, K., & O'Rourke, M. J. (1990). Seismic damage to segmented buried pipelines. *Earthquake Engineering & Structural Dynamics*, *19*(4), 529–539. https://doi.org/10.1002/eqe.4290190405

Flores-Berrones, R., & Liu, X. L. (2003). Seismic vulnerability of buried pipelines. *Geofisica Internacional*, *42*(2), 237–246. https://doi.org/10.22201/igeof.00167169p.2003.42.2.268

Kumar, A., Satyannarayana, R., & Rajesh, B. G. (2022). Correlation between SPT-N and shear wave velocity (VS) and seismic site classification for Amaravati city, India. *Journal of Applied Geophysics*, *205*(September 2021), 104757. https://doi.org/10.1016/j.jappgeo.2022.104757

Maotian, L., Xiaoling, Z., Qing, Y., & Ying, G. (2009). Numerical analysis of liquefaction of porous seabed around pipeline fixed in space under seismic loading. *Soil Dynamics and Earthquake Engineering*, *29*(5), 855–864. https://doi.org/10.1016/j.soildyn.2008.09.002

Midas GTS NX [340] v1.1 (2023). Geotechnical and Tunnel Analysis System reference manual for Modelling. In *Midas Corporation, Integrated Design and Analysis.*

Mishra, B. K. (2016). *Dynamic Response of Buried Pipelines — An Elasticity Solution*. *112*(August 1990), 291–295.

Nair, G. S., & Dash, S. R. (2015). *Review of Seismic Mitigation Techniques for Buried Pipelines in Fault Zones*. *December 2014*, 2794–2810.

Novak, M. (1974). Effect of soil on structural response to wind and earthquake. *Earthquake Engineering & Structural Dynamics*, *3*(1), 79–96. https://doi.org/10.1002/eqe.4290030107

Novak, M., & Hindy, A. (1980). *Seismic Analysis of Underground Tubular Structures.* (Vol. 8, pp. 287–294).

Saeedzadeh, R., & Hataf, N. (2011). Uplift response of buried pipelines in saturated sand deposit under earthquake loading. *Soil Dynamics and Earthquake Engineering*, *31*(10), 1378–1384. https://doi.org/10.1016/j.soildyn.2011.05.013

Tseng, W. C., Chien, L. K., Chuang, S. T., Tsai, P. C., Hsu, Y. T., Lu, T. T., & Lin, C. K. (2010). Stability assessment for the undersea gas pipeline. *Journal of Marine Science and Technology*, *18*(6), 809–818. https://doi.org/10.51400/2709-6998.1938

Umeda, Y. (2002). The 2000 western Tottori earthquake. *Earth, Planets and Space*, *54*(8), 54–55. https://doi.org/10.1186/BF03352073

Yan, S., Xu, Y. R., & Chang, H. Y. (2012). Numerical simulation of dynamic response of buried pipeline by ground explosion. *Earth and Space 2012 - Proceedings of the 13th ASCE Aerospace Division Conference and the 5th NASA/ASCE Workshop on Granular Materials in Space Exploration*, 1159–1166. https://doi.org/10.1061/9780784412190.126

Zhang, X. L., Jeng, D. S., & Luan, M. T. (2011). Dynamic response of a porous seabed around pipeline under three-dimensional wave loading. *Soil Dynamics and Earthquake Engineering*, *31*(5–6), 785–791. https://doi.org/10.1016/j.soildyn.2011.01.002